Development of Swinging Part Profilometer for Optics

Peng Zhang*[a], Jie Li[b], Guoyu Yu [a], David D. Walker [a,c,d]
[a]CPT, University of Huddersfield, OpTIC Centre, Ffordd William Morgan, St. Asaph Business Park, North Wales, UK, LL17 0JD; [b]Quality Inspection and Test Centre,The Institute of Optics and Electronics, Chengdu, China; [c]Dept. of Physics and Astronomy, University College London, London, UK, WC1E 6BT; [d]Zeeko Ltd, Coalville, UK, LE67 3FW

ABSTRACT

A new surface metrology instrument, the 'Swinging Part Profilometer' (SPP), has been developed for in-situ measurement of optics undergoing robot-processing in the ground (non-specular) state. In this paper, we present the hardware-design of the SPP, together with software for hardware-control, data-acquisition and surface-reconstruction. First results on a sample part are presented, compared with interferometric metrology, and error-contributions considered. Notably, during each individual scan of a measurement-cycle, the *probe remains fixed*. This lends itself to automated probe-deployment by the same robot as performs surface-processing, as probe stability is required on only the time-scale for a single scan.

1. INTRODUCTION

We have previously reported [1-3] on our on-going development of automated manufacturing cells for precision surfaces, which would ultimately contain CNC grinding, CNC polishing and metrology. We have considered a robot as a versatile device to provide dual-functionality – automating currently-manual functions on a Zeeko CNC polishing machine (or grinder), and providing in its own right an intermediate smoothing process-step between CNC grinding and polishing. In this paper, we consider how the metrology needed to support such an intermediate step can be delivered, leveraging the capabilities of a robot. This has led us to consider a new surface-metrology device, the "Swinging Part Profilometer" (SPP) for in-situ measurement.

The instrument is functionally a reversed version of a swinging-arm profilometer (SAP) [4-7]. In our case, the *work-piece* (not measurement arm) is mounted on a rotary air-bearing or hydrostatic table, which could be the turntable of a precision CNC grinding machine. Indeed, because the times for iterative CNC corrective polishing considerably exceed those for deterministic CNC grinding, the grinder turntable would be expected to have spare capacity. Alternatively, a separate metrology station could be installed in the Cell at additional capital cost.

In our concept, the workpiece can rotate either on-axis, or mechanically de-centred, with a moveable counter-weight under the workpiece to maintain turntable-balance. The probe remains stationery during a single scan, as the workpiece rotates on its axis or swings off-axis beneath it. The probe's lateral position (or, in principle, the workpiece de-centre) are then incremented before each successive scan. By this means, a series of scans of the workpiece can be built up, comprising on-axis concentric circles, intersecting de-centred arcs.

This mechanical configuration is particularly advantageous for robot processing cells, as the robot can automatically deploy polishing or smoothing tools or measurement probes, and is required to remain static and stable during only the individual times for each measurement-scan. The surface-form is then reconstructed from the assembly of several measurement scans, in a similar manner to the swinging-arm profilometer [8].

2. INSTRUMENT SETUP AND CHARACTERISATION

2.1 Instrument structure

The prototype SPP utilizes a rotary air-bearing turntable sitting on a granite table (Figure 1), which was originally built for measuring Wolter-type X-ray mirrors and mandrels [9], and kindly provided to us by Brera Observatory, Italy. We have re-conditioned the turntable rotary belt drive-system, and installed a new servo motor, encoder and electronics. This enables continuous rotation at a specified speed, incrementing through a specified angle, and controlled speed ramp-up/down. A rail-system is mounted on top of the rotary table, and is based on recirculating ball-bushings on precision stainless steel rails. The moving carriage supports a Y-shaped yoke, which in turn carries three contact pads (which could

Optics and Measurement International Conference 2016, edited by Jana Kovacicinova,
Proc. of SPIE Vol. 10151, 101510B · © 2016 SPIE · CCC code: 0277-786X/16/$18
doi: 10.1117/12.2256295

be extended to a whiffletree as required) to support the workpiece. The entire mechanism enables the workpiece to be positioned central on the air-bearing rotation-axis, or with a range of de-centres.

In the SAP, the angle between the arm's rotation-axis and the vertical is adjusted so that the probe describes a virtual sphere in space [4-6]. The setup is mechanically pre-adjusted so that this virtual sphere matches the best-fit sphere to the workpiece. This overcomes the re-entrant beam problem, in that a measurement beam from a vertical non-contact optical probe, striking a location on polished surface with significantly slope, will be reflected back away from the probe.

In the case of scattering surfaces such as we consider, the re-entrant beam problem is much less of an issue, so we can directly deploy various types of optical non-contact probes at a fixed (vertical) orientation in space [10]. In particular, we are using chromatic-aberration probes (CHRocodile chromatic optical probes, specifically the RB 200-071 with 10mm range and 300nm axial resolution. The other advantage of the SAP is that the measurement-range required of the probe is reduced to the misfit between aspheric surface and virtual sphere. In the SPP the full sag of the workpiece (or section of it to be measured) must be accommodated by the probe. However, as the instrument is targeted at the intermediate stage between CNC grinding and CNC polishing, we can deploy probes with less precision and greater range. In practice, the selected probe is mounted on the end of the arm of a standard ABB robot (type IRB 4600).

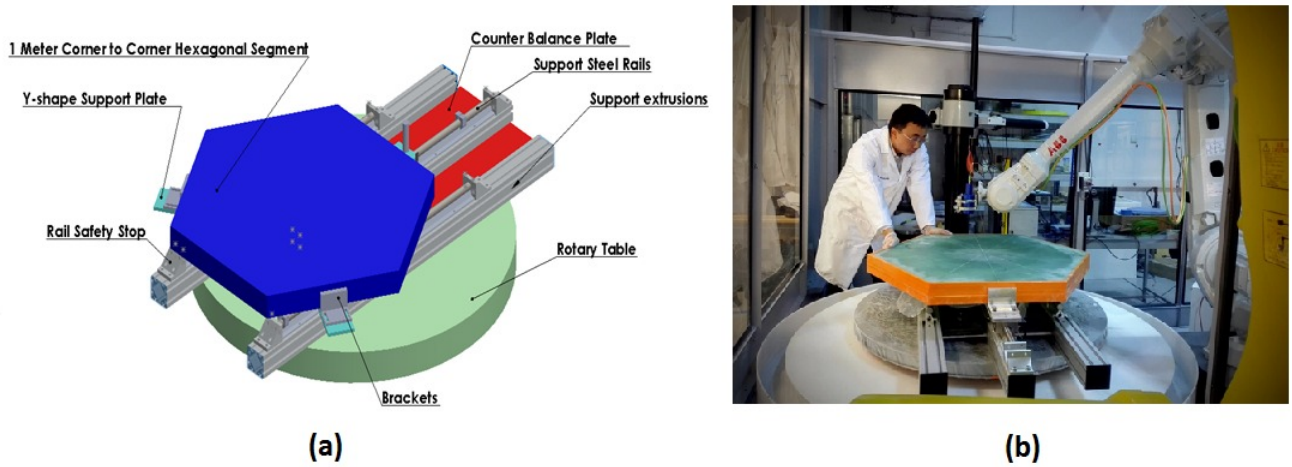

Figure 1. Swinging Part Profilometer; schematic design (a) and prototype (b)

2.2 Principles of the SPP

The basic data profiling pattern of the swinging part profilometer (SPP) is shown below (Figure 2), based on a vertical fixed probe held by the robot, as described above. Each full-circle scan is conducted by rotation of the turntable, incrementing the radial position of the probe using the ABB IRB 4600 robot between scans. This motion is not currently encoded, reliance being placed on the ~0.1mm accuracy delivered by the robot. To conduct the arcuate scans, the work-piece is then de-centred through a single fixed distance using the rail system. A moving counterweight underneath the work-piece yoke is then re-positioned to restore levelling and balance of the air-bearing turntable, using the robot-held probe. The family of arcuate scans is then conducted by rotating the turntable, and repeating after incrementing the probe lateral position.

Now, the measurement-precision associated with the each individual concentric circular scan is defined by the (high) precision of the air-bearing. However, the height-registration between scans is limited to the (lower) precision of the robot-positioning. The same applies to a set of arcuate scans. However, where a circular and arcuate scan intersects, the absolute height on the work-piece (in work-piece coordinates) must be identical. In an analogous manner to the SAP, the intersections between circular and concentric scans therefore give the additional information required to stitch the circular scans together. The relative height information among these circular profiles and their own errors are regarded as the total surface error of the work-piece. A Matlab program was coded to load, stitch and calculate the final surface error map, as that from SAP [11].

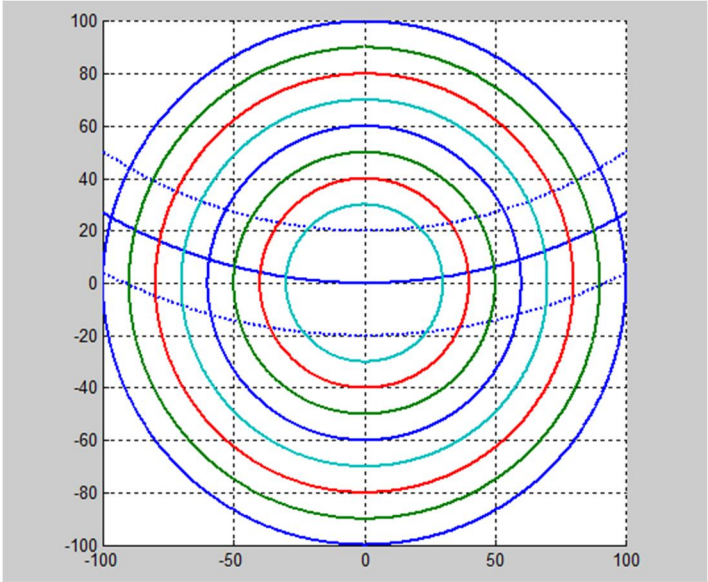

Figure 2. Example of an SPP profiling pattern.

2.3 Close loop test and environment characterization

The effect of lab temperature variations on the dimensional relationship between probe and work-piece is potentially important in the overall metrology error budget. To explore this, the probe and work-piece were left in contact but undisturbed for 18 hours, and probe-data collected and plotted (Figure 3a.) A periodic variation in both the probe's readings and temperature log was observed: the lab temperature cycling over ~ +/-1 ºC with a 30 minute period. The probe data (smaller-excursion line in Figure 3a) followed a similar pattern. This cycling is attributed to thermal expansion/contraction effects, in particular of the ABB robot arm. Fortunately, as seen in Figure 1b, the upward expansion of the main body of the robot is, to first approximation, compensated by the downward expansion of the arm itself.

In practice, the probe is required to remain at a fixed vertical relationship with respect to the work-piece during only a single scan. The typical single-scan time as currently configured is 150 seconds (full rotation of turntable). The typical slope in the probe-data of Figure 3 is then 3 microns/ ºC. From this, we estimate that the measurement height-error introduced by such a temperature excursion during a single scan, is 0.6 microns. This can in principle be reduced by running the turntable at a continuous, faster speed.

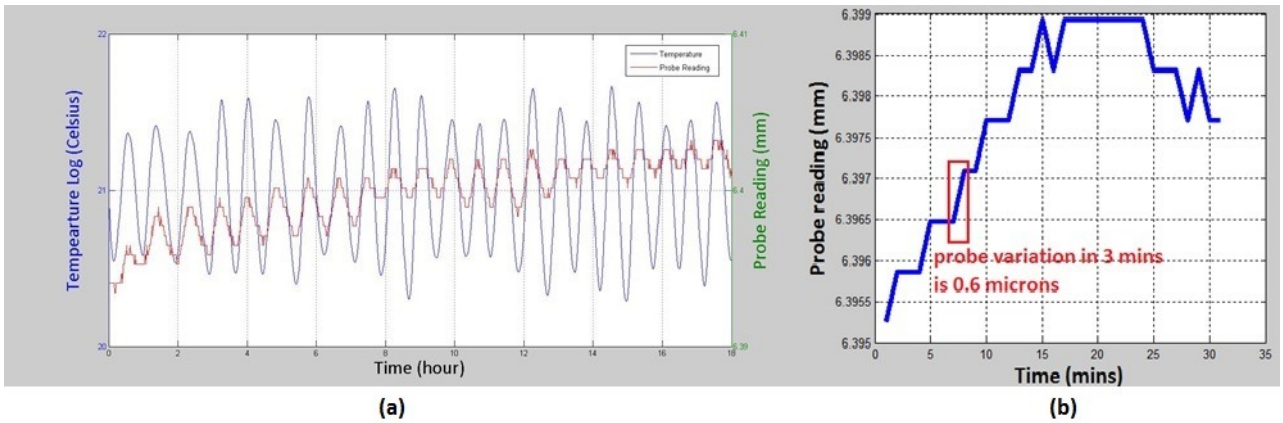

Figure 3. Environment characterization test within 18 hours.

2.4 Robot arm characterization

Next we consider in more detail the stability of the robot-mounted measurement probe during the period of each measurement scan. Given the 150 second typical rotation time of the turntable, we have collected static probe data over 3

minute periods. The probe data variation, attributed to vibration, was 0.6 μm PV (Figure 4), just twice the resolution of the probe used. The value of the probe data variation during 3 minutes (full rotation of rotary table) is consistent with the thermal drift (Figure 3b).

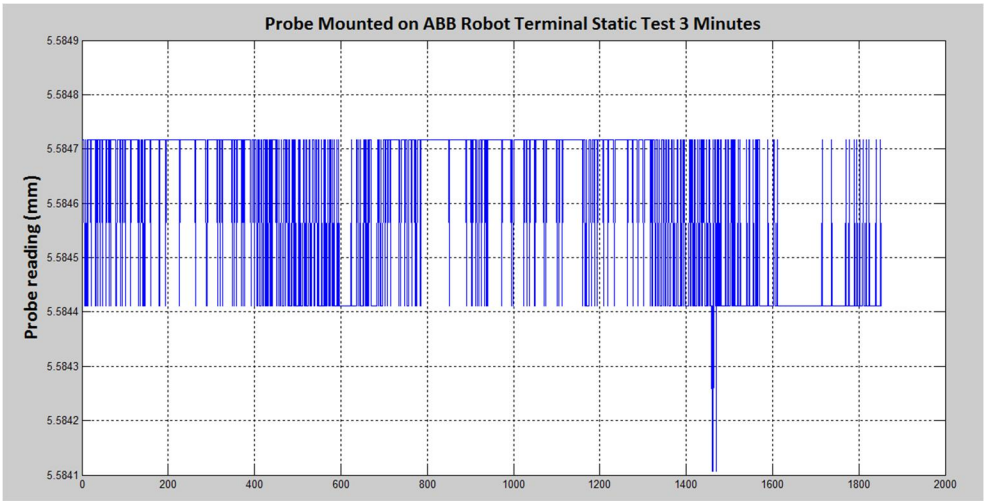

Figure 4. ABB Static Test in 3 Minutes.

3. DATA STITCHING

3.1 Principle of stitching

a. Calculate the 'best-fit' plane of each con-centric circle. Calculate the different value between real probe data and 'best-fit' plane data. Substitute this difference value for the probe data collected.
b. Measure the tilt angle change of the testing mirror surface when it is moved from centre to the de-centered position.
c. Rotate the arc scan data so that the arc can be parallel with the horizontal plane.
d. Calculate all the coordinates of intersection points between con-centric circles and one arc.
e. With the help of the intersection points coordinates, the vertical distance between each circle and the arc can be calculated. Because there are two intersection points between one circle and the arc, the arithmetic mean value of the two points is regarded as the distance between one circle and the arc.
f. Shift all the circle data based on the results from the previous step so that all the circle can be 'landed' on the arc scan.
g. Remove the arc data and the remaining con-centric circles data can represent the surface error map of the testing mirror.

3.2 Verification of stitching algorithm

It is important to verify the validation of the data stitching algorithm mentioned above. If a flat surface is being tested by SPP with a series of circular profiles and one arc scan, the final stitched surface error map should be or close to the flat plane. The p-v and rms error compared to the ideal flat plane should be zero. First of all, we generate eight concentric circles with different height in 3D space (Figure 5a). Each circular profile height is different because the non-contact probe is required to move from its current position to the adjacent point (Figure 5a). Then all the circle profiles are rotated with the X axis with a determined angle (Figure 5b). Let's assume that this tilt angle is $\pi/5000$. It is essential to conduct this data rotation since the testing work-piece is tilted. Similarly, a tilted arc profile data is also generated since the sliding rails will be bended slightly (48μm) when testing mirror is moved with 200mm (Figure 5c). Let's assume that the arc profile has a tilted angle of $\pi/5000+ \pi/10000$. On the final stage, all the circle profiles are translated along the Z axis and 'landed' on the arc scan profile (Figure 5d). The error of each circle profile and their relative height information determine the final error map of the testing mirror.

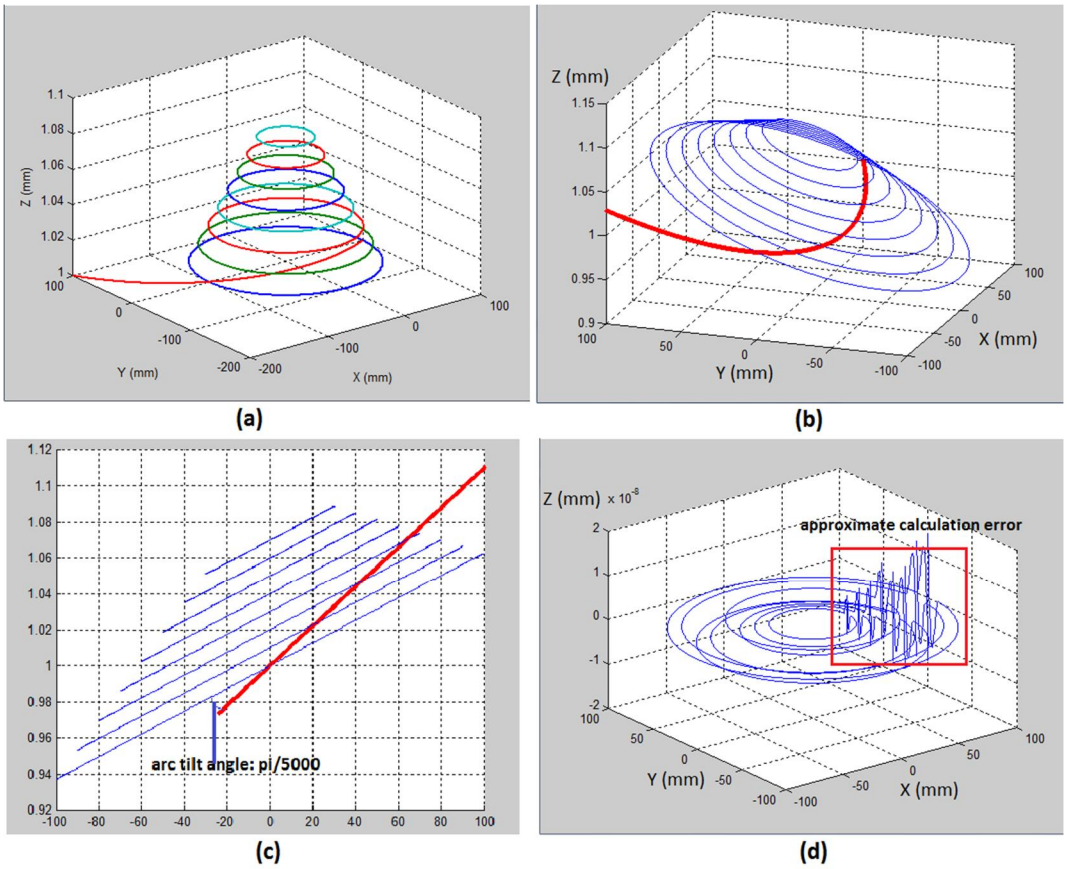

Figure 5. Data Stitching Algorithm (a, b, c, d).

A Matlab program was coded in order or load and calculate the stitched result (Figure 6). The calculated final stitched result is: root mean square (rms) is 2.09×10^{-6} μm and peak-to-valley (p-v) is 6.49×10^{-6} μm. The unit scale is 10^{-6}μm is 0.001 nm which is extremely close to the ideal flat surface. The existence of nonzero rms and p-v error is because the approximate calculation by Matlab software. This calculated surface error map can confirm that the data stitching algorithm is right and trusted.

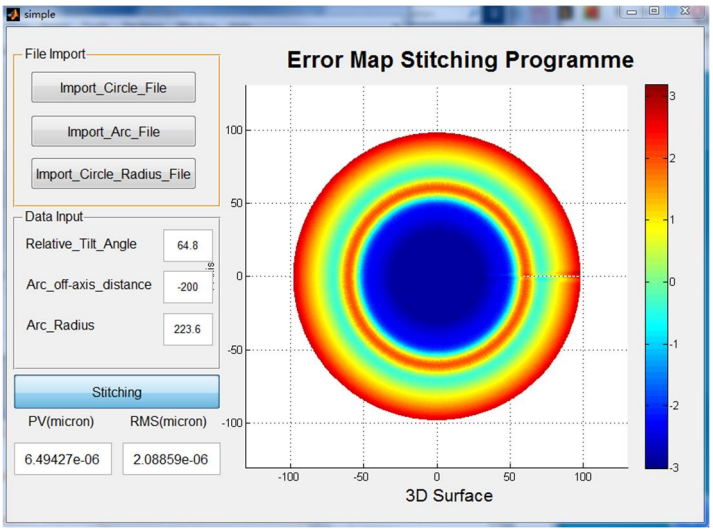

Figure 6. Validation Result of Generated Data.

4. EXPERIMENT AND DATA ANALYSIS

4.1 Experiment Set up

As a first demonstration, a plano work-piece with aperture 300mm was tested. This was polished to facilitate comparative metrology using an interferometer. The work-piece was placed directly onto the centre of a 1 meter hexagonal ground part already on the profilometer, providing a convenient base. Seven concentric profiles were measured (Table 1).

Table 1. Con-centric circles and arc scan parameters.

Circle Radius (mm)	90	80	70	60	50	40	30
Arc scan radius (mm)		200		Arc scan swing angle (degree)		52.01	

The different radii of the circular profiles were defined tracking the probe light-spot over a pre-made template. The ABB robot was used to move the probe to each of the eight defined starting points. Matlab software synchronised and controlled rotation of the air-bearing table and the probe data-collection. The work-piece was then moved 200mm from the axial to decentered position, along the sliding rails and the air-bearing re-balanced. The rotary table was programmed to rotate through a scanning arc of 15 degree, sufficient for the probe to intersect twice each of the complete family of concentric scans.

The acceleration and deceleration of the rotary table can introduce positional and height errors into the probe data, when measuring the arc profile. In order to minimize this, the table was rotated through seven continuous revolutions. Data from revolutions 1,2,6,7 were discarded, 3,4,5 being averaged and the tip/tilt terms removed. The arcuate scan data (solid line Figure 7) was compared with interferometer data from a linear cross-section of the part (dashed line Figure 7). The linear trace was orientated tangent to the arcuate scan at the centre of the part, and so these scans sampled similar, but not identical, tracks across the surface. The interferometer linear scan gave 178nm pv and the averaged SPP arcuate scan190nm. Given the probe's stated resolution of 300nm, the discrepancy was significantly better than expected, providing a sound basis for using the arcuate SPP data in stitching on this, a nominally flat surface.

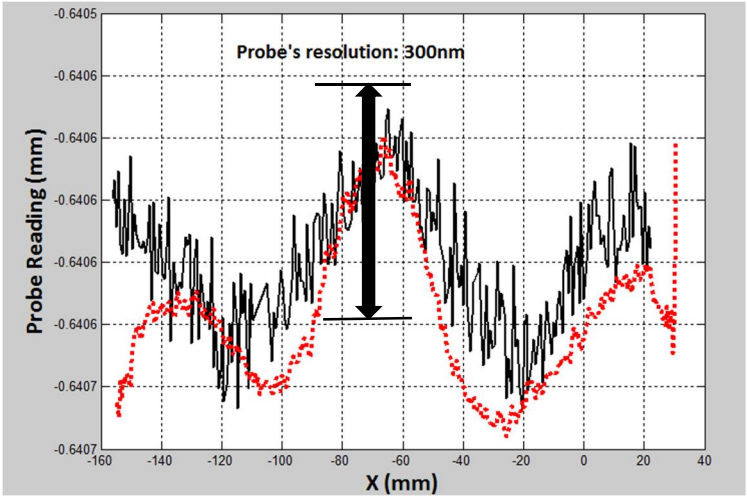

Figure 7. Compare the SPP averaged arc raw data with interferometer cross-section data (solid line: SPP arc, dashed line: interferometer)

Raw data (Figure 8a) of all the con-centric circles were filtered to remove noise (Figure 8b), then loaded into a Matlab stitching program to reconstruct the work-piece surface-map.

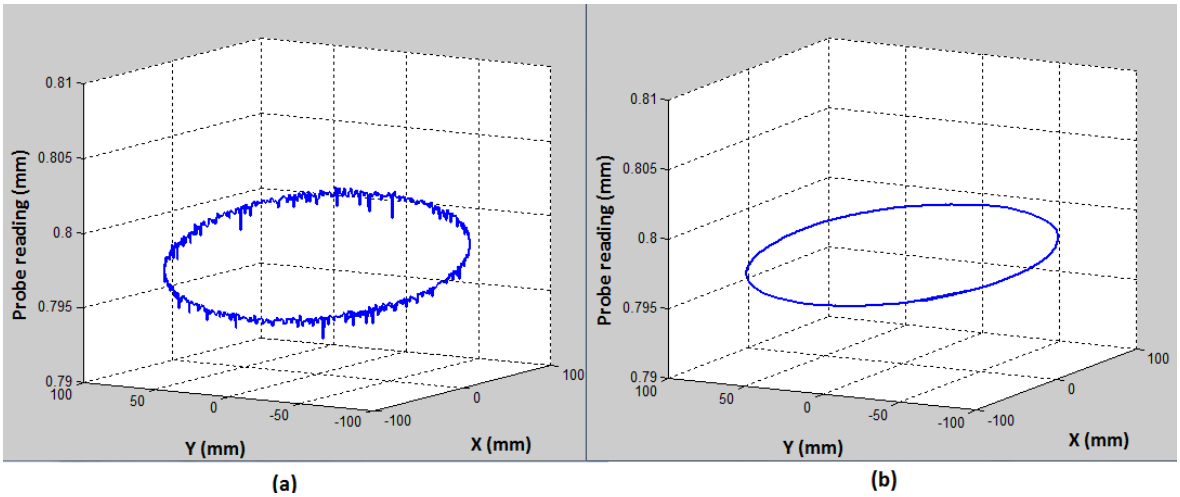

Figure 8. Data Filter (left: raw data; right: filtered data)

The stitched error map of the testing work-piece with aperture 180mm with PV error of 355nm and RMS error of 55nm. The work-piece was also measured by interferometer which shows the PV error of 190nm and RMS error of 31nm (Figure 9).

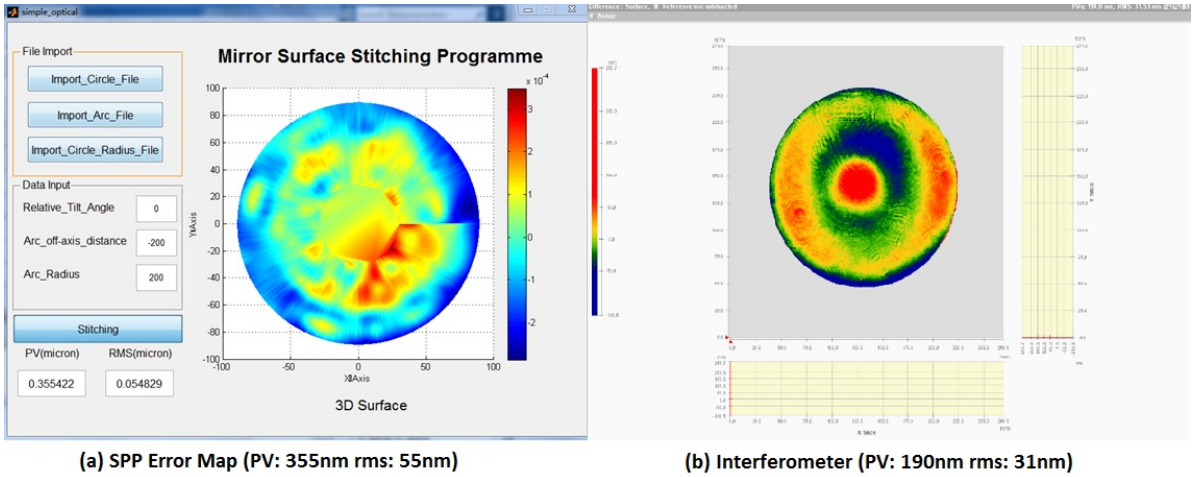

Figure 9. Comparision of metrology on a testing surface of aperture 180 mm. (a) stitched data with PV error of 355nm and RMS error of 55nm and (b) measured from interferometer with PV error of 190nm and RMS error of 31nm.

5. CONCLUSIONS

The Swinging Part Profilometer is potentially well suited to incorporation in a Manufacturing Cell to provide speedy metrology of surfaces in the ground state, which are undergoing smoothing and low-order correction between CNC grinding and CNC polishing. This suitability is the more apparent given that grinding times are much shorter than corrective polishing, releasing the precision turntable of a CNC grinder to support SPP operation at no extra capital cost.

We have reported on the successful completion of a prototype profilometer based on an existing and available air bearing turntable. In this prototype, the part-under-test can rotate on-axis on the air-bearing turntable, or displaced off-axis. A standard robot has been shown to provide adequate stability to hold a height-probe in a stationery position during each of the individual scans invoked by turntable-rotation, providing that thermal drift is managed by keeping the scan-time short. Incrementing the probe position between scans enables measurements of concentric circles, and offsetting the part as well, intersecting concentric arcs. Moving the probe between scans using the robot introduces significant height discrepancies.

However, by analogy with the swinging-arm profilometer, the surface topography can be reconstructed using the intersections between circular and arcuate scans. We have developed software to command turntable rotation, measure encoder feedback and acquire probe data in a synchronized manner; also stitching software to reconstruct the surface.

We have presented first results measuring a nominal flat, and performance appears to exceed the advertised 300nm resolution of the probe. Our planned future work will progress to curved and ultimately free-form surfaces, together with detailed quantification and management of errors of measurement. Curved surface measurements will undoubtedly more challenging, as results will be sensitive to air-bearing run-out, robot lateral position accuracy etc. We plan to use the uncertainty budget as the main tool in exploring, quantifying, and allowing for these types of effects.

REFERENCES

[1] Walker, David D., et al. "Closing the metrology/process loop in CNC polishing." *Third European Seminar on Precision Optics Manufacturing*. International Society for Optics and Photonics, 2016.

[2] Walker, D. D., et al. "Robotic automation in computer controlled polishing." *Journal of the European Optical Society-Rapid publications* 11 (2016).

[3] Walker, David, et al. "The role of robotics in computer controlled polishing of large and small optics." *SPIE Optical Engineering+ Applications*. International Society for Optics and Photonics, 2015.

[4] Wang, Yuhao, et al. "Swing arm optical coordinate-measuring machine: high precision measuring ground aspheric surfaces using a laser triangulation probe." *Optical Engineering* 51.7 (2012): 073603-1.

[5] Su, Peng, et al. "Swing arm optical CMM: self calibration with dual probe shear test." *SPIE Optical Engineering+ Applications*. International Society for Optics and Photonics, 2011.

[6] Su, Peng, et al. "Swing arm optical CMM for aspherics." *SPIE Optical Engineering+ Applications*. International Society for Optics and Photonics, 2009.

[7] Alejandro V. Maldonado, Peng Su, and James H. Burge, "Development of a portable deflectometry system for high spatial resolution surface measurements," Appl. Opt. 53, 4023-4032 (2014).

[8] Dae Wook Kim ; ByoungChang Kim ; Chunyu Zhao ; ChangJin Oh ; James H. Burge; Algorithms for surface reconstruction from curvature data for freeform aspherics. Proc. SPIE 8838, Optical Manufacturing and Testing X, 88380B (September 7, 2013); doi:10.1117/12.2024285.

[9] Kwon Su Chon, Yoshiharu Namba, and Kwon-Ha Yoon, "Wolter type I x-ray focusing mirror using multilayer coatings," Appl. Opt. 45, 4609-4616 (2006).

[10] Lee, Dong-Hyeok. "3-Dimensional profile distortion measured by stylus type surface profilometer." Measurement 46.1 (2013): 803-814.

[11] Chen, Shanyong, et al. "Error analysis and surface reconstruction for swing arm profilometry." *Measurement* 87 (2016): 1-12.